Evidence for a Neutral Near-Threshold Structure in the K_S^0 Recoil-Mass Spectra in $e^+e^- \to K_S^0 D_s^+ D^{*-}$ and $e^+e^- \to K_S^0 D_s^{*+} D^-$

M. Ablikim,[1] M. N. Achasov,[11,b] P. Adlarson,[70] M. Albrecht,[4] R. Aliberti,[31] A. Amoroso,[69a,69c] M. R. An,[35] Q. An,[66,53] X. H. Bai,[61] Y. Bai,[52] O. Bakina,[32] R. Baldini Ferroli,[26a] I. Balossino,[27a] Y. Ban,[42,g] V. Batozskaya,[1,40] D. Becker,[31] K. Begzsuren,[29] N. Berger,[31] M. Bertani,[26a] D. Bettoni,[27a] F. Bianchi,[69a,69c] J. Bloms,[63] A. Bortone,[69a,69c] I. Boyko,[32] R. A. Briere,[5] A. Brueggemann,[63] H. Cai,[71] X. Cai,[1,53] A. Calcaterra,[26a] G. F. Cao,[1,58] N. Cao,[1,58] S. A. Cetin,[57a] J. F. Chang,[1,53] W. L. Chang,[1,58] G. Chelkov,[32,a] C. Chen,[39] Chao Chen,[50] G. Chen,[1] H. S. Chen,[1,58] M. L. Chen,[1,53] S. J. Chen,[38] S. M. Chen,[56] T. Chen,[1] X. R. Chen,[28,58] X. T. Chen,[1] Y. B. Chen,[1,53] Z. J. Chen,[23,h] W. S. Cheng,[69c] X. Chu,[39] G. Cibinetto,[27a] F. Cossio,[69c] J. J. Cui,[45] H. L. Dai,[1,53] J. P. Dai,[73] A. Dbeyssi,[17] R. E. de Boer,[4] D. Dedovich,[32] Z. Y. Deng,[1] A. Denig,[31] I. Denysenko,[32] M. Destefanis,[69a,69c] F. De Mori,[69a,69c] Y. Ding,[36] J. Dong,[1,53] L. Y. Dong,[1,58] M. Y. Dong,[1,53,58] X. Dong,[71] S. X. Du,[75] P. Egorov,[32,a] Y. L. Fan,[71] J. Fang,[1,53] S. S. Fang,[1,58] W. X. Fang,[1] Y. Fang,[1] R. Farinelli,[27a] L. Fava,[69b,69c] F. Feldbauer,[4] G. Felici,[26a] C. Q. Feng,[66,53] J. H. Feng,[54] K. Fischer,[64] M. Fritsch,[4] C. Fritzsch,[63] C. D. Fu,[1] H. Gao,[58] Y. N. Gao,[42,g] Yang Gao,[66,53] S. Garbolino,[69c] I. Garzia,[27a,27b] P. T. Ge,[71] Z. W. Ge,[38] C. Geng,[54] E. M. Gersabeck,[62] A. Gilman,[64] K. Goetzen,[12] L. Gong,[36] W. X. Gong,[1,53] W. Gradl,[31] M. Greco,[69a,69c] L. M. Gu,[38] M. H. Gu,[1,53] Y. T. Gu,[14] C. Y. Guan,[1,58] A. Q. Guo,[28,58] L. B. Guo,[37] R. P. Guo,[44] Y. P. Guo,[10,f] A. Guskov,[32,a] T. T. Han,[45] W. Y. Han,[35] X. Q. Hao,[18] F. A. Harris,[60] K. K. He,[50] K. L. He,[1,58] F. H. Heinsius,[4] C. H. Heinz,[31] Y. K. Heng,[1,53,58] C. Herold,[55] M. Himmelreich,[12,d] G. Y. Hou,[1,58] Y. R. Hou,[58] Z. L. Hou,[1] H. M. Hu,[1,58] J. F. Hu,[51,i] T. Hu,[1,53,58] Y. Hu,[1] G. S. Huang,[66,53] K. X. Huang,[54] L. Q. Huang,[67] L. Q. Huang,[28,58] X. T. Huang,[45] Y. P. Huang,[1] Z. Huang,[42,g] T. Hussain,[68] N. Hüsken,[25,31] W. Imoehl,[25] M. Irshad,[66,53] J. Jackson,[25] S. Jaeger,[4] S. Janchiv,[29] Q. Ji,[1] Q. P. Ji,[18] X. B. Ji,[1,58] X. L. Ji,[1,53] Y. Y. Ji,[45] Z. K. Jia,[66,53] H. B. Jiang,[45] S. S. Jiang,[35] X. S. Jiang,[1,53,58] Y. Jiang,[58] J. B. Jiao,[45] Z. Jiao,[21] S. Jin,[38] Y. Jin,[61] M. Q. Jing,[1,58] T. Johansson,[70] N. Kalantar-Nayestanaki,[59] X. S. Kang,[36] R. Kappert,[59] M. Kavatsyuk,[59] B. C. Ke,[75] I. K. Keshk,[4] A. Khoukaz,[63] P. Kiese,[31] R. Kiuchi,[1] R. Kliemt,[12] L. Koch,[33] O. B. Kolcu,[57a] B. Kopf,[4] M. Kuemmel,[4] M. Kuessner,[4] A. Kupsc,[40,70] W. Kühn,[33] J. J. Lane,[62] J. S. Lange,[33] P. Larin,[17] A. Lavania,[24] L. Lavezzi,[69a,69c] Z. H. Lei,[66,53] H. Leithoff,[31] M. Lellmann,[31] T. Lenz,[31] C. Li,[43] C. Li,[39] C. H. Li,[35] Cheng Li,[66,53] D. M. Li,[75] F. Li,[1,53] G. Li,[1] H. Li,[47] H. Li,[66,53] H. B. Li,[1,58] H. J. Li,[18] H. N. Li,[51,i] J. Q. Li,[4] J. S. Li,[54] J. W. Li,[45] Ke Li,[1] L. J. Li,[1] L. K. Li,[1] Lei Li,[3] M. H. Li,[39] P. R. Li,[34,j,k] S. X. Li,[10] S. Y. Li,[56] T. Li,[45] W. D. Li,[1,58] W. G. Li,[1] X. H. Li,[66,53] X. L. Li,[45] Xiaoyu Li,[1,58] H. Liang,[66,53] H. Liang,[1,58] H. Liang,[30] Y. F. Liang,[49] Y. T. Liang,[28,58] G. R. Liao,[13] L. Z. Liao,[45] J. Libby,[24] A. Limphirat,[55] C. X. Lin,[54] D. X. Lin,[28,58] T. Lin,[1] B. J. Liu,[1] C. X. Liu,[1] D. Liu,[17,66] F. H. Liu,[48] Fang Liu,[1] Feng Liu,[6] G. M. Liu,[51,i] H. Liu,[34,j,k] H. B. Liu,[14] H. M. Liu,[1,58] Huanhuan Liu,[1] Huihui Liu,[19] J. B. Liu,[66,53] J. L. Liu,[67] J. Y. Liu,[1,58] K. Liu,[1] K. Y. Liu,[36] Ke Liu,[20] L. Liu,[66,53] Lu Liu,[39] M. H. Liu,[10,f] P. L. Liu,[1] Q. Liu,[58] S. B. Liu,[66,53] T. Liu,[10,f] W. K. Liu,[39] W. M. Liu,[66,53] X. Liu,[34,j,k] Y. Liu,[34,j,k] Y. B. Liu,[39] Z. A. Liu,[1,53,58] Z. Q. Liu,[45] X. C. Lou,[1,53,58] F. X. Lu,[54] H. J. Lu,[21] J. G. Lu,[1,53] X. L. Lu,[1] Y. Lu,[7] Y. P. Lu,[1,53] Z. H. Lu,[1] C. L. Luo,[37] M. X. Luo,[74] T. Luo,[10,f] X. L. Luo,[1,53] X. R. Lyu,[58] Y. F. Lyu,[39] F. C. Ma,[36] H. L. Ma,[1] L. L. Ma,[45] M. M. Ma,[1,58] Q. M. Ma,[1] R. Q. Ma,[1,58] R. T. Ma,[58] X. Y. Ma,[1,53] Y. Ma,[42,g] F. E. Maas,[17] M. Maggiora,[69a,69c] S. Maldaner,[4] S. Malde,[64] Q. A. Malik,[68] A. Mangoni,[26a] Y. J. Mao,[42,g] Z. P. Mao,[1] S. Marcello,[69a,69c] Z. X. Meng,[61] J. G. Messchendorp,[59,12] G. Mezzadri,[27a] H. Miao,[1] T. J. Min,[38] R. E. Mitchell,[25] X. H. Mo,[1,53,58] N. Yu. Muchnoi,[11,b] Y. Nefedov,[32] F. Nerling,[17,d] I. B. Nikolaev,[11,b] Z. Ning,[1,53] S. Nisar,[9,l] Y. Niu,[45] S. L. Olsen,[58] Q. Ouyang,[1,53,58] S. Pacetti,[26b,26c] X. Pan,[10,f] Y. Pan,[52] A. Pathak,[30] M. Pelizaeus,[4] H. P. Peng,[66,53] K. Peters,[12,d] J. L. Ping,[37] R. G. Ping,[1,58] S. Plura,[31] S. Pogodin,[32] V. Prasad,[66,53] F. Z. Qi,[1] H. Qi,[66,53] H. R. Qi,[56] M. Qi,[38] T. Y. Qi,[10,f] S. Qian,[1,53] W. B. Qian,[58] Z. Qian,[54] C. F. Qiao,[58] J. J. Qin,[67] L. Q. Qin,[13] X. P. Qin,[10,f] X. S. Qin,[45] Z. H. Qin,[1,53] J. F. Qiu,[1] S. Q. Qu,[39] S. Q. Qu,[56] K. H. Rashid,[68] C. F. Redmer,[31] K. J. Ren,[35] A. Rivetti,[69c] V. Rodin,[59] M. Rolo,[69c] G. Rong,[1,58] Ch. Rosner,[17] S. N. Ruan,[39] H. S. Sang,[66] A. Sarantsev,[32,c] Y. Schelhaas,[31] C. Schnier,[4] K. Schoenning,[70] M. Scodeggio,[27a,27b] K. Y. Shan,[10,f] W. Shan,[22] X. Y. Shan,[66,53] J. F. Shangguan,[50] L. G. Shao,[1,58] M. Shao,[66,53] C. P. Shen,[10,f] H. F. Shen,[1,58] X. Y. Shen,[1,58] B. A. Shi,[58] H. C. Shi,[66,53] J. Y. Shi,[1] q. q. Shi,[50] R. S. Shi,[1,58] X. Shi,[1,53] X. D. Shi,[66,53] J. J. Song,[18] W. M. Song,[30,1] Y. X. Song,[42,g] S. Sosio,[69a,69c] S. Spataro,[69a,69c] F. Stieler,[31] K. X. Su,[71] P. P. Su,[50] Y. J. Su,[58] G. X. Sun,[1] H. Sun,[58] H. K. Sun,[1] J. F. Sun,[18] L. Sun,[71] S. S. Sun,[1,58] T. Sun,[1,58] W. Y. Sun,[30] X. Sun,[23,h] Y. J. Sun,[66,53] Y. Z. Sun,[1] Z. T. Sun,[45] Y. H. Tan,[71] Y. X. Tan,[66,53] C. J. Tang,[49] G. Y. Tang,[1] J. Tang,[54] L. Y. Tao,[67] Q. T. Tao,[23,h] M. Tat,[64] J. X. Teng,[66,53] V. Thoren,[70] W. H. Tian,[47] Y. Tian,[28,58] I. Uman,[57b] B. Wang,[1] B. L. Wang,[58] C. W. Wang,[38] D. Y. Wang,[42,g] F. Wang,[67] H. J. Wang,[34,j,k] H. P. Wang,[1,58] K. Wang,[1,53] L. L. Wang,[1] M. Wang,[45] M. Z. Wang,[42,g] Meng Wang,[1,58]

S. Wang,[13] S. Wang,[10,f] T. Wang,[10,f] T. J. Wang,[39] W. Wang,[54] W. H. Wang,[71] W. P. Wang,[66,53] X. Wang,[42,g] X. F. Wang,[34,j,k] X. L. Wang,[10,f] Y. Wang,[56] Y. D. Wang,[41] Y. F. Wang,[1,53,58] Y. H. Wang,[43] Y. Q. Wang,[1] Yaqian Wang,[16,1] Z. Wang,[1,53] Z. Y. Wang,[1,58] Ziyi Wang,[58] D. H. Wei,[13] F. Weidner,[63] S. P. Wen,[1] D. J. White,[62] U. Wiedner,[4] G. Wilkinson,[64] M. Wolke,[70] L. Wollenberg,[4] J. F. Wu,[1,58] L. H. Wu,[1] L. J. Wu,[1,58] X. Wu,[10,f] X. H. Wu,[30] Y. Wu,[66] Y. J. Wu,[28] Z. Wu,[1,53] L. Xia,[66,53] T. Xiang,[42,g] D. Xiao,[34,j,k] G. Y. Xiao,[38] H. Xiao,[10,f] S. Y. Xiao,[1] Y. L. Xiao,[10,f] Z. J. Xiao,[37] C. Xie,[38] X. H. Xie,[42,g] Y. Xie,[45] Y. G. Xie,[1,53] Y. H. Xie,[6] Z. P. Xie,[66,53] T. Y. Xing,[1,58] C. F. Xu,[1] C. J. Xu,[54] G. F. Xu,[1] H. Y. Xu,[61] Q. J. Xu,[15] X. P. Xu,[50] Y. C. Xu,[58] Z. P. Xu,[38] F. Yan,[10,f] L. Yan,[10,f] W. B. Yan,[66,53] W. C. Yan,[75] H. J. Yang,[46,e] H. L. Yang,[30] H. X. Yang,[1] L. Yang,[47] S. L. Yang,[58] Tao Yang,[1] Y. F. Yang,[39] Y. X. Yang,[1,58] Yifan Yang,[1,58] M. Ye,[1,53] M. H. Ye,[8] J. H. Yin,[1] Z. Y. You,[54] B. X. Yu,[1,53,58] C. X. Yu,[39] G. Yu,[1,58] T. Yu,[67] C. Z. Yuan,[1,58] L. Yuan,[2] S. C. Yuan,[1] X. Q. Yuan,[1] Y. Yuan,[1,58] Z. Y. Yuan,[54] C. X. Yue,[35] A. A. Zafar,[68] F. R. Zeng,[45] X. Zeng,[6] Y. Zeng,[23,h] Y. H. Zhan,[54] A. Q. Zhang,[1] B. L. Zhang,[1] B. X. Zhang,[1] D. H. Zhang,[39] G. Y. Zhang,[18] H. Zhang,[66] H. H. Zhang,[54] H. H. Zhang,[30] H. Y. Zhang,[1,53] J. L. Zhang,[72] J. Q. Zhang,[37] J. W. Zhang,[1,53,58] J. X. Zhang,[34,j,k] J. Y. Zhang,[1] J. Z. Zhang,[1,58] Jianyu Zhang,[1,58] Jiawei Zhang,[1,58] L. M. Zhang,[56] L. Q. Zhang,[54] Lei Zhang,[38] P. Zhang,[1] Q. Y. Zhang,[35,75] Shuihan Zhang,[1,58] Shulei Zhang,[23,h] X. D. Zhang,[41] X. M. Zhang,[1] X. Y. Zhang,[45] X. Y. Zhang,[50] Y. Zhang,[64] Y. T. Zhang,[75] Y. H. Zhang,[1,53] Yan Zhang,[66,53] Yao Zhang,[1] Z. H. Zhang,[1] Z. Y. Zhang,[71] Z. Y. Zhang,[39] G. Zhao,[1] J. Zhao,[35] J. Y. Zhao,[1,58] J. Z. Zhao,[1,53] Lei Zhao,[66,53] Ling Zhao,[1] M. G. Zhao,[39] Q. Zhao,[1] S. J. Zhao,[75] Y. B. Zhao,[1,53] Y. X. Zhao,[28,58] Z. G. Zhao,[66,53] A. Zhemchugov,[32,a] B. Zheng,[67] J. P. Zheng,[1,53] Y. H. Zheng,[58] B. Zhong,[37] C. Zhong,[67] X. Zhong,[54] H. Zhou,[45] L. P. Zhou,[1,58] X. Zhou,[71] X. K. Zhou,[58] X. R. Zhou,[66,53] X. Y. Zhou,[35] Y. Z. Zhou,[10,f] J. Zhu,[39] K. Zhu,[1] K. J. Zhu,[1,53,58] L. X. Zhu,[58] S. H. Zhu,[65] S. Q. Zhu,[38] T. J. Zhu,[72] W. J. Zhu,[10,f] Y. C. Zhu,[66,53] Z. A. Zhu,[1,58] B. S. Zou,[1] and J. H. Zou[1]

(BESIII Collaboration)

[1]*Institute of High Energy Physics, Beijing 100049, People's Republic of China*
[2]*Beihang University, Beijing 100191, People's Republic of China*
[3]*Beijing Institute of Petrochemical Technology, Beijing 102617, People's Republic of China*
[4]*Bochum Ruhr-University, D-44780 Bochum, Germany*
[5]*Carnegie Mellon University, Pittsburgh, Pennsylvania 15213, USA*
[6]*Central China Normal University, Wuhan 430079, People's Republic of China*
[7]*Central South University, Changsha 410083, People's Republic of China*
[8]*China Center of Advanced Science and Technology, Beijing 100190, People's Republic of China*
[9]*COMSATS University Islamabad, Lahore Campus, Defence Road, Off Raiwind Road, 54000 Lahore, Pakistan*
[10]*Fudan University, Shanghai 200433, People's Republic of China*
[11]*G.I. Budker Institute of Nuclear Physics SB RAS (BINP), Novosibirsk 630090, Russia*
[12]*GSI Helmholtzcentre for Heavy Ion Research GmbH, D-64291 Darmstadt, Germany*
[13]*Guangxi Normal University, Guilin 541004, People's Republic of China*
[14]*Guangxi University, Nanning 530004, People's Republic of China*
[15]*Hangzhou Normal University, Hangzhou 310036, People's Republic of China*
[16]*Hebei University, Baoding 071002, People's Republic of China*
[17]*Helmholtz Institute Mainz, Staudinger Weg 18, D-55099 Mainz, Germany*
[18]*Henan Normal University, Xinxiang 453007, People's Republic of China*
[19]*Henan University of Science and Technology, Luoyang 471003, People's Republic of China*
[20]*Henan University of Technology, Zhengzhou 450001, People's Republic of China*
[21]*Huangshan College, Huangshan 245000, People's Republic of China*
[22]*Hunan Normal University, Changsha 410081, People's Republic of China*
[23]*Hunan University, Changsha 410082, People's Republic of China*
[24]*Indian Institute of Technology Madras, Chennai 600036, India*
[25]*Indiana University, Bloomington, Indiana 47405, USA*
[26a]*INFN Laboratori Nazionali di Frascati, I-00044, Frascati, Italy*
[26b]*INFN Sezione di Perugia, I-06100, Perugia, Italy*
[26c]*University of Perugia, I-06100, Perugia, Italy*
[27a]*INFN Sezione di Ferrara, I-44122, Ferrara, Italy*
[27b]*University of Ferrara, I-44122, Ferrara, Italy*
[28]*Institute of Modern Physics, Lanzhou 730000, People's Republic of China*
[29]*Institute of Physics and Technology, Peace Avenue 54B, Ulaanbaatar 13330, Mongolia*
[30]*Jilin University, Changchun 130012, People's Republic of China*
[31]*Johannes Gutenberg University of Mainz, Johann-Joachim-Becher-Weg 45, D-55099 Mainz, Germany*

[32]Joint Institute for Nuclear Research, 141980 Dubna, Moscow region, Russia
[33]Justus-Liebig-Universitaet Giessen, II. Physikalisches Institut, Heinrich-Buff-Ring 16, D-35392 Giessen, Germany
[34]Lanzhou University, Lanzhou 730000, People's Republic of China
[35]Liaoning Normal University, Dalian 116029, People's Republic of China
[36]Liaoning University, Shenyang 110036, People's Republic of China
[37]Nanjing Normal University, Nanjing 210023, People's Republic of China
[38]Nanjing University, Nanjing 210093, People's Republic of China
[39]Nankai University, Tianjin 300071, People's Republic of China
[40]National Centre for Nuclear Research, Warsaw 02-093, Poland
[41]North China Electric Power University, Beijing 102206, People's Republic of China
[42]Peking University, Beijing 100871, People's Republic of China
[43]Qufu Normal University, Qufu 273165, People's Republic of China
[44]Shandong Normal University, Jinan 250014, People's Republic of China
[45]Shandong University, Jinan 250100, People's Republic of China
[46]Shanghai Jiao Tong University, Shanghai 200240, People's Republic of China
[47]Shanxi Normal University, Linfen 041004, People's Republic of China
[48]Shanxi University, Taiyuan 030006, People's Republic of China
[49]Sichuan University, Chengdu 610064, People's Republic of China
[50]Soochow University, Suzhou 215006, People's Republic of China
[51]South China Normal University, Guangzhou 510006, People's Republic of China
[52]Southeast University, Nanjing 211100, People's Republic of China
[53]State Key Laboratory of Particle Detection and Electronics, Beijing 100049, Hefei 230026, People's Republic of China
[54]Sun Yat-Sen University, Guangzhou 510275, People's Republic of China
[55]Suranaree University of Technology, University Avenue 111, Nakhon Ratchasima 30000, Thailand
[56]Tsinghua University, Beijing 100084, People's Republic of China
[57a]Turkish Accelerator Center Particle Factory Group, Istinye University, 34010, Istanbul, Turkey
[57b]Near East University, Nicosia, North Cyprus, Mersin 10, Turkey
[58]University of Chinese Academy of Sciences, Beijing 100049, People's Republic of China
[59]University of Groningen, NL-9747 AA Groningen, The Netherlands
[60]University of Hawaii, Honolulu, Hawaii 96822, USA
[61]University of Jinan, Jinan 250022, People's Republic of China
[62]University of Manchester, Oxford Road, Manchester, M13 9PL, United Kingdom
[63]University of Muenster, Wilhelm-Klemm-Strasse 9, 48149 Muenster, Germany
[64]University of Oxford, Keble Road, Oxford OX13RH, United Kingdom
[65]University of Science and Technology Liaoning, Anshan 114051, People's Republic of China
[66]University of Science and Technology of China, Hefei 230026, People's Republic of China
[67]University of South China, Hengyang 421001, People's Republic of China
[68]University of the Punjab, Lahore-54590, Pakistan
[69a]University of Turin, I-10125, Turin, Italy
[69b]University of Eastern Piedmont, I-15121, Alessandria, Italy
[69c]INFN, I-10125, Turin, Italy
[70]Uppsala University, Box 516, SE-75120 Uppsala, Sweden
[71]Wuhan University, Wuhan 430072, People's Republic of China
[72]Xinyang Normal University, Xinyang 464000, People's Republic of China
[73]Yunnan University, Kunming 650500, People's Republic of China
[74]Zhejiang University, Hangzhou 310027, People's Republic of China
[75]Zhengzhou University, Zhengzhou 450001, People's Republic of China

(Received 26 April 2022; revised 17 June 2022; accepted 30 June 2022; published 9 September 2022)

We study the processes $e^+e^- \to K_S^0 D_s^+ D^{*-}$ and $e^+e^- \to K_S^0 D_s^{*+} D^-$, as well as their charge conjugated processes, at five center-of-mass energies between 4.628 and 4.699 GeV, using data samples corresponding to an integrated luminosity of 3.8 fb^{-1} collected by the BESIII detector at the BEPCII storage ring. Based on a partial reconstruction technique, we find evidence of a structure near the thresholds for $D_s^+ D^{*-}$ and $D_s^{*+} D^-$ production in the K_S^0 recoil-mass spectrum, which we refer to as the $Z_{cs}(3985)^0$. Fitting with a

Breit-Wigner line shape, we find the mass of the structure to be $(3992.2 \pm 1.7 \pm 1.6)\ \mathrm{MeV}/c^2$ and the width to be $(7.7^{+4.1}_{-3.8} \pm 4.3)$ MeV, where the first uncertainties are statistical and the second are systematic. The significance of the $Z_{cs}(3985)^0$ signal is found to be 4.6σ including both the statistical and systematic uncertainty. We report the Born cross section multiplied by the branching fraction at different energy points. The mass of the $Z_{cs}(3985)^0$ is close to that of the $Z_{cs}(3985)^+$. Assuming SU(3) symmetry, the cross section of the neutral channel is consistent with that of the charged one. Hence, we conclude that the $Z_{cs}(3985)^0$ is the isospin partner of the $Z_{cs}(3985)^+$.

DOI: 10.1103/PhysRevLett.129.112003

Extensive evidence exists for several nonstrange hidden-charm tetraquark Z_c candidates, with quark constituent of $c\bar{c}q\bar{q}'$ ($q^{(\prime)} = u$ or d) [1–4]. In electron-positron annihilation, both charged and neutral $Z_c(3900)$ and $Z_c(4020)$ states have been observed by the BESIII, Belle, and CLEO collaborations [5–15]. Under SU(3) flavor symmetry, one expects the existence of corresponding strange partners with $c\bar{c}s\bar{q}$ configurations, denoted as Z_{cs} states [16]. These Z_{cs} states are predicted to have masses close to the $D_s\bar{D}^*$ and $D_s^*\bar{D}$ thresholds in a variety of models explaining their nature, including the tetraquark scenario [17,18], the molecular model [19], the hadron-quarkonium model [18], and the initial single chiral particle emission mechanism [20].

The charged-tetraquark candidate $Z_{cs}(3985)^+$ [21] was observed at BESIII in the $D_s^+\bar{D}^{*0}$ and $D_s^{*+}\bar{D}^0$ final states [22–26]. The mass of the $Z_{cs}(3985)^+$ is close to the $D_s^+\bar{D}^{*0}$ and $D_s^{*+}\bar{D}^0$ thresholds, which is consistent with theoretical predictions [17–20]. Meanwhile, another charged-tetraquark candidate, $Z_{cs}(4000)^+$ [27], was observed in the $J/\psi K^+$ final states in an amplitude analysis of the decay $B^+ \to J/\psi \phi K^+$ at LHCb. However, the widths of these two Z_{cs}^+ states are inconsistent with each other. The observation of these charged Z_{cs} states motivates a search for a neutral isospin partner Z_{cs}^0. The mass of the Z_{cs}^0 is expected to be heavier than that of the Z_{cs}^+ by $(0.05 \pm 0.21)\ \mathrm{GeV}/c^2$ under the molecular hypothesis, or by $(0.06 \pm 0.12)\ \mathrm{GeV}/c^2$ under the tetraquark hypothesis [23]. A promising approach to this challenge at BESIII is to search for the process $e^+e^- \to \bar{K}^0 Z_{cs}(3985)^0 +$ c.c. and then compare its cross section to that of $e^+e^- \to K^- Z_{cs}(3985)^+ +$ c.c., which tests the isospin symmetry in the production and decay dynamics. A similar strategy was pursued in the analysis of the Z_c charged and neutral states [10,11]. Observation and study of the Z_{cs}^0 is crucial for understanding the nature of the Z_{cs} states.

In this Letter, we study the processes $e^+e^- \to K_S^0 D_s^+ D^{*-}$ and $e^+e^- \to K_S^0 D_s^{*+} D^-$, which is denoted as $e^+e^- \to K_S^0(D_s^+D^{*-} + D_s^{*+}D^-)$ in the context, as well as their charge conjugated modes, using e^+e^- collision datasets corresponding to an integrated luminosity of 3.8 fb^{-1} [28] at center-of-mass energies $\sqrt{s} = 4.628$, 4.641, 4.661, 4.682, and 4.699 GeV [28]. These samples were collected by the BESIII detector at the Beijing Electron Positron Collider (BEPCII). Detailed information about BEPCII and BESIII can be found in Refs. [29–31]. We use a partial reconstruction technique to maximize the detection efficiency; only the K_S^0 produced in association with the $D_s^+D^{*-}$ or $D_s^{*+}D^-$ (the "bachelor" K_S^0) and one of the ground-state D mesons (here D subsequently denotes D_s^+ or D^-) are detected, while the other final-state particles are not reconstructed. The Z_{cs}^0 candidate is then searched for in the invariant mass distribution recoiling against the bachelor K_S^0 candidate. Charge conjugation is implied throughout the discussion.

Simulated samples produced with a GEANT4-based [32] Monte Carlo (MC) package, which includes the geometric description of the BESIII detector and the detector response, are used to determine the detection efficiency and to understand the backgrounds. The e^+e^- annihilations are simulated with the KKMC [33] generator, which includes the effects of the beam-energy spread and initial-state radiation. The inclusive MC sample consists of the production of open-charm hadronic systems, initial-state radiation production of vector charmonium(-like) states, and continuum processes incorporated in KKMC [33]. The known decay modes are modeled with EVTGEN [34] using branching fractions reported by the Particle Data Group (PDG) [35], and the remaining unknown decays from charmonium states are modeled with LUNDCHARM [36]. The final-state radiation from charged final-state particles is simulated with the PHOTOS package [37]. For the nonresonant three-body signal processes $e^+e^- \to K_S^0(D_s^+D^{*-} + D_s^{*+}D^-)$, the momenta distributions of final-state particles are generated following phase space. For the resonant signal process $e^+e^- \to K_S^0 Z_{cs}^0 \to K_S^0(D_s^+D^{*-} + D_s^{*+}D^-)$, we assume that the Z_{cs}^0 state has a spin parity of 1^+, which corresponds to S waves in both of the decays $e^+e^- \to K_S^0 Z_{cs}^0$ and $Z_{cs}^0 \to D_s^+D^{*-} + D_s^{*+}D^-$, which we denote as (S, S). The corresponding angular distribution is taken into account in simulating the cascade decays. Other possibilities for the Z_{cs}^0 spin parity are tested to evaluate the systematic uncertainty related to this assumption.

We carry out two types of partial reconstruction, which are referred as the D_s^+-tag and D^--tag methods, respectively. For $D_s^+(D^-)$-tag method, only the bachelor K_S^0 and $D_s^+(D^-)$ candidates are reconstructed. We use the decay modes $D_s^+ \to K^+K^-\pi^+$, $K_S^0K^+$, $K^+K^-\pi^+\pi^0$, $K_S^0K^+\pi^+\pi^-$, and $\eta'\pi^+$ to form the D_s^+ candidates; and the decay modes $D^- \to K^+\pi^-\pi^-$, $K_S^0\pi^-$, and $K_S^0\pi^+\pi^-\pi^-$ to form the D^- candidates.

To ensure that each charged track, which is not associated to K_S^0 detection, originates from the e^+e^- interaction point (IP), $|V_r| < 1$ cm and $|V_z| < 10$ cm are required. Here, $|V_r|$ is the distance between the charged track and the beam axis in the transverse plane, and $|V_z|$ is the closest distance of the charged track to the IP along the axis of beam. The polar angles of charged tracks are required to satisfy $|\cos\theta| < 0.93$. The flight time in the time-of-flight system and the energy deposited in the multilayer drift chamber for each charged track are used to identify particles by calculating the probabilities $P(i)$, where i denotes K or π. We require $P(K)$ $[P(\pi)]$ to be greater than $P(\pi)$ $[P(K)]$ to classify a particle as a kaon (pion) candidate.

The K_S^0 candidates are reconstructed through the $\pi^+\pi^-$ decay mode without particle identification requirements. Both pions must satisfy $|V_z| < 20$ cm, and $|\cos\theta| < 0.93$ and their trajectories are constrained to originate from a common vertex by applying a vertex fit, the χ^2 of which is required to be less than 100. The K_S^0 candidate is then formed and the opposite direction of its momentum is constrained to point at the IP, with the corresponding χ^2 required to be less than 40. The decay length of K_S^0 candidate must be > 2 standard deviations of the vertex resolution away from the IP. The invariant mass of $\pi^+\pi^-$ pair, $M(\pi^+\pi^-)$, is required to be within $(0.492, 0.503)$ GeV/c^2.

The π^0 and η candidates are reconstructed through $\pi^0/\eta \to \gamma\gamma$. The photon showers in the electromagnetic calorimeter must have energies greater than 25 MeV in the barrel region ($|\cos\theta| < 0.80$) and greater than 50 MeV in the end-cap region ($0.86 < |\cos\theta| < 0.92$). Showers must have an associated time within 700 ns of the event start time. A kinematic fit is applied to constrain the invariant mass of the $\gamma\gamma$ pair to the known π^0 or η mass reported in the PDG [35], and the resultant χ^2 is required to be less than 10. The η' is reconstructed through $\eta' \to \pi^+\pi^-\eta$. The mass of the $\pi^+\pi^-\eta$ is required to be within 10 MeV/c^2 of the known η' [35] mass.

To improve the signal purity, the requirements listed in Table I are adopted to restrict the final states within the regions of the ϕ, K^*, and ρ resonances, which dominate the decays. In the selection of $D^- \to K_S^0\pi^+\pi^-\pi^-$ candidates, contamination from the decay $D^- \to K_S^0K_S^0\pi^-$ is suppressed by requiring the invariant mass of the $\pi^+\pi^-$ pair to lie outside the interval $(0.48, 0.52)$ GeV/c^2. To avoid double counting and to suppress backgrounds, we only keep the D_s^+ (D^-) candidate with an invariant mass closest to the known D_s^+ (D^-) mass. In the invariant-mass spectra of the D decay final states, the signal candidates are selected by requiring the reconstructed mass $M(D)$ to be within 15 MeV/c^2 of the known mass of the charm meson in question. The $M(D_s^+)$ sideband regions are defined as $(1.895, 1.935)$ GeV/c^2 and $(1.995, 2.035)$ GeV/c^2, while the $M(D^-)$ sideband regions are defined as $(1.800, 1.840)$ GeV/c^2 and $(1.900, 1.940)$ GeV/c^2, which are taken as control samples for studying the combinatorial backgrounds in the subsequent analysis.

The recoil mass $RM(K_S^0D)$ of the K_S^0D system is obtained according to $RM(X) = \|p_{e^+e^-} - p_X\|$, where $p_{e^+e^-}$ is the four-momentum of the initial e^+e^- system and p_X is the four-momentum of the X system. The $RM(K_S^0D)$ resolution is then improved through use of the quantity $RQ(K_S^0D) = RM(K_S^0D) + M(D) - m(D)$ [38], where $M(D)$ is the invariant mass of the signal D candidate, and $m(D)$ is the known mass quoted in PDG

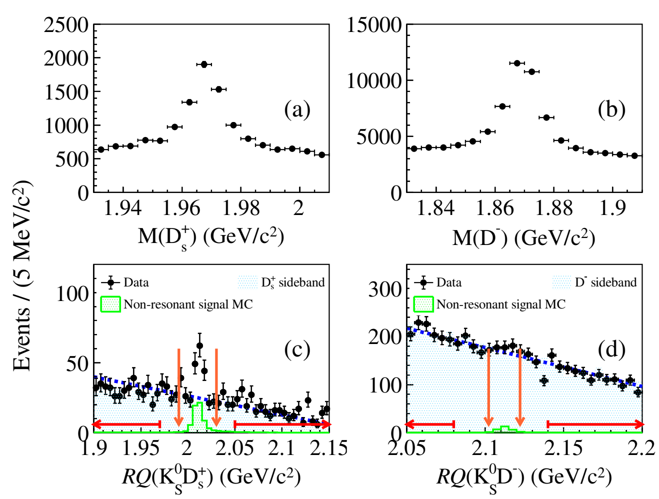

FIG. 1. Invariant-mass distributions of the singly tagged D_s^+ (a) and D^- (b), together with the fits to the recoil-mass distributions $RQ(K_S^0D_s^+)$ (c) and $RQ(K_S^0D^-)$ (d) at 4.682 GeV. The points with error bars are data. The blue-dashed lines show the fit results of the sideband regions, which are denoted by the red arrows. The histograms show the distributions from the nonresonant signal MC samples, which are scaled according to the yields of D^{*-} and D_s^{*+}. The orange arrows indicate the signal regions of the D^{*-} in (c) and D_s^{*+} in (d).

TABLE I. Summary of the cuts applied to the D_s^+ and D^- decay modes for the combinatorial background suppression. Here, M denotes the reconstructed invariant mass and m the known mass.

Final state	Requirement
$D_s^+ \to K^+K^-\pi^+$	$M(K^+K^-) < 1.05$ GeV/c^2 $\lvert M(K^+\pi^-) - m[K^*(892)]\rvert < 70$ MeV/c^2
$D_s^+ \to K^+K^-\pi^+\pi^0$	$M(K^+K^-) < 1.05$ GeV/c^2 $\lvert M(\pi^-\pi^0) - m(\rho)\rvert < 150$ MeV/c^2
$D_s^+ \to K_S^0K^+\pi^+\pi^-$	$\lvert M(K^+\pi^-) - m[K^*(892)]\rvert < 70$ MeV/c^2
$D^- \to K_S^0\pi^+\pi^-\pi^-$	$\lvert M(K_S^0\pi^+) - m[K^*(892)]\rvert < 70$ MeV/c^2

TABLE II. Number of combinatorial background candidates in the signal regions of the $K_S^0 D_s^+ D^{*-}$ and $K_S^0 D_s^{*+} D^-$ three-body processes.

$\sqrt{s}$ (MeV)	D_s^+-tag	D^--tag
4628	40.6 ± 3.4	132.1 ± 6.1
4641	49.8 ± 3.7	169.1 ± 6.8
4661	57.5 ± 4.0	184.3 ± 6.9
4682	199.0 ± 7.3	668.8 ± 12.9
4699	68.6 ± 4.2	217.5 ± 7.4

[35]. The $RQ(K_S^0 D)$ spectra are shown in Fig. 1. These spectra are used to identify the three-body processes $K_S^0 D_s^+ D^{*-}$ and $K_S^0 D_s^{*+} D^-$, which contribute to peaking structures in the regions of the D^{*-} and D_s^{*+} mass, respectively. We require $|RQ(K_S^0 D_s^+) - m(D^{*-})| < 20\ \mathrm{MeV}/c^2$ and $|RQ(K_S^0 D^-) - m(D_s^{*+})| < 10\ \mathrm{MeV}/c^2$. Studies of the inclusive MC simulations show that there is negligible peaking background in the signal regions. To evaluate the level of combinatorial background in the sample of selected three-body candidates, linear fits to the $RQ(K_S^0 D_s^+)$ sideband region ($[1.90, 1.97]\ \mathrm{GeV}/c^2$ and $[2.05, 2.15]\ \mathrm{GeV}/c^2$), and to the $RQ(K_S^0 D^-)$ sideband region ($[2.05, 2.08]\ \mathrm{GeV}/c^2$ and $[2.14, 2.20]\ \mathrm{GeV}/c^2$) are performed, where the slopes are fixed according to the corresponding $M(D)$ sideband samples. Table II lists the number of combinatorial background candidates for the two tag methods at each energy point.

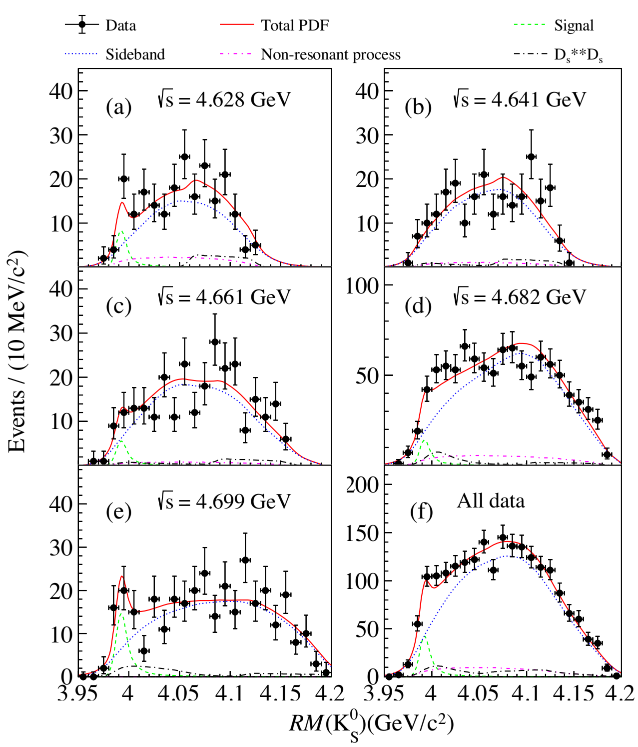

FIG. 2. Simultaneous fit to the recoil-mass $RM(K_S^0)$ spectra in all datasets [(a)–(e)], and for all the data points combined (f). The green dashed curves show the Z_{cs}^0 signal contribution. The pink dash-dotted curves show the nonresonant process. The blue dotted curves show combinatorial backgrounds. The black long dash-dotted curves show contributions from the highly excited $D_{(s)}^{**}$ backgrounds.

Figure 2 shows $RM(K_S^0)$, the bachelor K_S^0 recoil-mass distribution, for the signal candidates selected from both tags. There is an enhancement near the mass threshold of $D_s^+ D^{*-}$ and $D_s^{*+} D^-$, which is most evident in the 4.682 GeV and 4.699 GeV datasets.

To understand potential contributions from the highly excited strange-charmed mesons D_s^{**} in the $RM(K_S^0)$ distribution, we simulate the exclusive production of $D_{s1}(2536)^- D_s^+$, $D_{s2}(2573)^- D_s^{*+}$, and $D_{s1}(2700)^- D_s^+$ in e^+e^- annihilations. Assuming isospin symmetry, their production cross sections are those of the corresponding states studied during the analysis of the charged $Z_{cs}(3985)^+$ [21]. In addition, the potential effect of excited nonstrange charmed mesons D^{**} are explored as described in Ref. [39], where $D_2^*(2460)^+ D^{*-}$, $D(2550)^+ D^-$, $D_1^*(2600)^+ D^{*-}$, $D_1^*(2600)^+ D^-$, $D(2740)^+ D^-$, and $D_3^*(2750)^+ D^-$ are taken into account. We find the threshold enhancement cannot be explained by these excited states, and hence, we consider its possible origin to be the neutral Z_{cs}^0 state.

A simultaneous unbinned maximum likelihood fit is applied to the distributions of $RM(K_S^0)$ at five energy points. We adopt two S-wave Breit-Wigner functions R_1 and R_2 to describe the Z_{cs}^0 resonance:

$$R = \left| \frac{1}{M^2 - m_0^2 + i m_0 [f \cdot \Gamma_1(M) + (1-f) \cdot \Gamma_2(M)]} \right|^2$$

$$R_1 = R \cdot q \cdot p_1, \qquad R_2 = R \cdot q \cdot p_2,$$

$$\Gamma_1(M) = \Gamma_0 \cdot \frac{p_1}{p_1^*} \cdot \frac{m_0}{M}, \qquad \Gamma_2(M) = \Gamma_0 \cdot \frac{p_2}{p_2^*} \cdot \frac{m_0}{M},$$

where R_1 describes the decay $Z_{cs}^0 \to D_s^+ D^{*-}$, and R_2 describes $Z_{cs}^0 \to D_s^{*+} D^-$, M equals $RM(K_S^0)$, m_0 is the mass of the Z_{cs}^0, and Γ_0 is the total width of the Z_{cs}^0. The momentum of the K_S^0 in the initial e^+e^- system is q, the momentum of the $D_s^+(D^-)$ in the rest frame of the $D_s^+ D^{*-}(D_s^{*+} D^-)$ system is $p_{1(2)}$, and the corresponding momentum at $M = m_0$ is $p_{1(2)}^*$. In the fit, under the assumption of the isospin symmetry, a Gaussian constraint is imposed to restrict the width of the Z_{cs}^0 within the uncertainty of the $Z_{cs}(3985)^+$ width, which is $(13.8^{+8.1}_{-5.2} \pm 4.9)$ MeV [21]. The factor f denotes the ratio of the two signal channels:

$$f = \frac{\mathcal{B}(Z_{cs}^0 \to D_s^+ D^{*-})}{\mathcal{B}(Z_{cs}^0 \to D_s^+ D^{*-}) + \mathcal{B}(Z_{cs}^0 \to D_s^{*+} D^-)}. \qquad (1)$$

TABLE III. The measured masses and widths of the $Z_{cs}(3985)^0$ and $Z_{cs}(3985)^+$ [21].

	Mass (MeV/c^2)	Width (MeV)
$Z_{cs}(3985)^0$	$3992.2 \pm 1.7 \pm 1.6$	$7.7^{+4.1}_{-3.8} \pm 4.3$
$Z_{cs}(3985)^+$	$3985.2^{+2.1}_{-2.0} \pm 1.7$	$13.8^{+8.1}_{-5.2} \pm 4.9$

The default value of f is chosen to be 0.5, with other possibilities considered as a systematic uncertainty.

The fit depends on the detector resolution and mass-dependent efficiency, which are derived from simulated samples. The detector resolution is determined using the Z_{cs}^0 signal MC samples, in which the width of the Z_{cs}^0 is set to be 0. The signal probability density function (PDF) is constructed as follows:

$$\mathcal{F} \propto (f \cdot \mathcal{E}_1 \cdot R_1 + (1-f) \cdot \mathcal{E}_2 \cdot R_2) \otimes G(\mu, \sigma), \quad (2)$$

where $\mathcal{E}_{1(2)}$ is the efficiency function and G is the Gaussian resolution function.

The backgrounds in the fit include three components: the nonresonant process $e^+e^- \to K_S^0(D_s^+D^{*-} + D_s^{*+}D^-)$, the excited $D_s^{**}D_s$ backgrounds, and the combinatorial backgrounds. The first and second components are described using histogram PDFs extracted from MC samples, and the third component is described using the distribution from the D_s^+ (D^-) sideband. In the fit, the yields of the excited $D_s^{**}D_s$ backgrounds are estimated from isospin relations according to those calculated for the $e^+e^- \to K^-Z_{cs}(3985)^+$ process, and the numbers are fixed in the fit [21], while the yields of the nonresonant process are free. The sizes of the combinatorial background are fixed to the values in Table II.

The fitted mass and width of the Z_{cs}^0 are given in Table III, where the $Z_{cs}(3985)^+$ resonance parameters are included for comparison. The results are consistent with the theoretical predictions [17–20,23]. We sum up the $RM(K_S^0)$ distributions from all datasets, and superimpose the simultaneous fit curves in the last plot of Fig. 2. Comparing the fits with or without considering the contribution from the Z_{cs}^0, the number of degrees of freedom is changed by 7 (the mass and width of the Z_{cs}^0, together with the cross section of the Z_{cs}^0 at the five center-of-mass energies). The value of $2\ln L$, where L is the likelihood value, is changed by 42.0. This corresponds to a statistical significance of 5.0σ according to Wilks' theorem [40]. When also considering systematic uncertainties, which are described in the Supplemental Material [39], the significance of the Z_{cs}^0 signal becomes 4.6σ. The reduced chi-squared of the fit in Fig. 2 is 0.9, indicating good compatibility between the model and the data.

According to the fitted signal yields in Table IV, the Born cross section of $e^+e^- \to \bar{K}^0Z_{cs}^0$ multiplied by the branching fraction of Z_{cs}^0 decays, $\sigma^{\text{Born}}(e^+e^- \to \bar{K}^0Z_{cs}^0 + \text{c.c.}) \times \mathcal{B}(Z_{cs}^0 \to D_s^+D^{*-} + D_s^{*+}D^-)$, can be obtained by the following equation:

$$\sigma^{\text{Born}} \times \mathcal{B} = \frac{N^{\text{obs}}}{2\mathcal{L} \times \hat{\epsilon} \times (1+\delta) \times \delta_{\text{vac}}}, \quad (3)$$

where N^{obs} are the signal yields, $\hat{\epsilon}$ are the combined MC-determined reconstruction efficiencies in the two D-tag methods, $\mathcal{L}$ is the integrated luminosity, $(1+\delta)$ is the radiative correction factor, and δ_{vac} is the vacuum-polarization correction factor [41]; their values are given in Table IV. We assume $\mathcal{B}(Z_{cs}^0 \to D_s^+D^{*-}) = \mathcal{B}(Z_{cs}^0 \to D_s^{*+}D^-)$. The factor of 2 in the denominator in Eq. (3) is necessary because of the equal transition rate of K^0 and $\bar{K}^0$ to K_S^0. The cross section results at the five center-of-mass energies are listed in Table V. The χ^2 of each energy point is defined as the square of difference of the cross sections of two channels divided by the sum of squares of these uncertainties. The $\chi^2_{\text{total}}/\text{ndf}$ is the sum of the χ^2 divided by the number of energy points. The cross section results for the neutral channel are consistent with those for the charged one [21], which agree with the prediction based on isospin symmetry.

Systematic uncertainties on the measurement of the Z_{cs}^0 resonance parameters and production cross sections are

TABLE IV. Summary of the integrated luminosity ($\mathcal{L}$), the number of signal events (N^{obs}), reconstruction efficiency ($\hat{\epsilon}$), radiative-correction factor $(1+\delta)$, and vacuum polarization factor (δ_{vac}).

$\sqrt{s}$ (MeV)	$\mathcal{L}$ (pb^{-1})	N^{obs}	$\hat{\epsilon}(\%)$	$(1+\delta)\delta_{\text{vac}}$
4628	511.1	$14.4^{+8.9}_{-7.5}$	1.88	0.69
4641	541.4	$0.0^{+5.8}_{-0.0}$	1.88	0.74
4661	523.6	$10.0^{+6.9}_{-5.9}$	1.83	0.77
4682	1643.4	$25.5^{+13.6}_{-11.4}$	1.80	0.79
4699	526.2	$26.1^{+8.4}_{-7.5}$	1.78	0.80

TABLE V. Born cross sections multiplied by branching fraction of $\bar{K}^0Z_{cs}(3985)^0$ and $K^-Z_{cs}(3985)^+$ at the five energy points. The χ^2/ndf quantifies the compatibility of the five measurements.

	$\sigma^{\text{Born}} \times \mathcal{B}$(pb)			
$\sqrt{s}$ (MeV)	$\bar{K}^0Z_{cs}(3985)^0$	$K^-Z_{cs}(3985)^+$	χ^2	$\chi^2_{\text{total}}/\text{ndf}$
4628	$4.4^{+2.6}_{-2.2} \pm 2.0$	$0.8^{+1.2}_{-0.8} \pm 0.6$	1.2	
4641	$0.0^{+1.6}_{-0.0} \pm 0.2$	$1.6^{+1.2}_{-1.1} \pm 1.3$	0.5	
4661	$2.8^{+1.8}_{-1.6} \pm 0.6$	$1.6^{+1.3}_{-1.1} \pm 0.8$	0.3	5.1/5
4682	$2.2^{+1.2}_{-1.0} \pm 0.8$	$4.4^{+0.9}_{-0.8} \pm 1.4$	1.0	
4699	$7.0^{+2.2}_{-2.0} \pm 1.8$	$2.4^{+1.1}_{-1.0} \pm 1.2$	2.1	

extensively investigated as detailed in Ref. [39]. An important contribution is associated with the background modeling in the fit and the Z_{cs}^0 signal model. For the background modeling, we vary the size and shape of the combinatorial backgrounds according to the $M(D)$ side-band control samples, as well as explore the additional contributions from the highly excited $D_{(s)}^{**}$ states. For the signal modeling, we test different J^P assignments of the Z_{cs}^0 by changing the matrix elements in the signal simulations. The total systematic uncertainties are, overall, similar to the statistical uncertainties on each measurement.

In summary, based on datasets with center-of-mass energies from 4.628 to 4.699 GeV at BESIII, evidence of a neutral open-strange hidden-charm state, $Z_{cs}(3985)^0$, is found in the K_S^0 recoil-mass spectrum of the $e^+e^- \to K_S^0(D_s^+D^{*-} + D_s^{*+}D^-) + \text{c.c.}$ processes, with a resonance mass and width determined as $(3992.2 \pm 1.7 \pm 1.6)\ \text{MeV}/c^2$ and $(7.7^{+4.1}_{-3.8} \pm 4.3)$ MeV, respectively. The significance of the state is determined to be 4.6σ. Since this state decays through $D_s^+D^{*-}$ and $D_s^{*+}D^-$, it should contain at least four quarks, $c\bar{c}\bar{s}d$. The measured mass of the $Z_{cs}(3985)^0$ is larger than that of the $Z_{cs}(3985)^+$, which is consistent with theoretical prediction [23]. In addition, the Born cross sections of $e^+e^- \to \bar{K}^0 Z_{cs}(3985)^0 + \text{c.c.}$ multiplied by the branching fraction of $Z_{cs}(3985)^0 \to D_s^+D^{*-} + D_s^{*+}D^-$ at the five energy points are measured and found to be consistent with those of $e^+e^- \to K^- Z_{cs}(3985)^+ + \text{c.c.}$ [21], as is expected under isospin symmetry. Hence, we conclude that the $Z_{cs}(3985)^0$ is the isospin partner of the $Z_{cs}(3985)^+$.

The BESIII collaboration thanks the staff of BEPCII and the IHEP computing center for their strong support. This work is supported in part by National Key R&D Program of China under Contracts No. 2020YFA0406400, 2020YFA0406300; National Natural Science Foundation of China (NSFC) under Contracts No. 11521505, 11635010, 11735014, 11805086, 11822506, 11835012, 11935015, 11935016, 11935018, 11961141012, 12022510, 12025502, 12035009, 12035013; National 1000 Talents Program of China; the Chinese Academy of Sciences (CAS) Large-Scale Scientific Facility Program; Joint Large-Scale Scientific Facility Funds of the NSFC and CAS under Contract No. U1832207; CAS Key Research Program of Frontier Sciences under Contract No. QYZDJ-SSW-SLH040; 100 Talents Program of CAS; Fundamental Research Funds for the Central Universities, Lanzhou University, University of Chinese Academy of Sciences; INPAC and Shanghai Key Laboratory for Particle Physics and Cosmology; ERC under Contract No. 758462; European Union Horizon 2020 research and innovation programme under Contract No. Marie Sklodowska-Curie grant agreement no. 894790; German Research Foundation DFG under Contracts No. 443159800, Collaborative Research Center CRC 1044, FOR 2359, GRK 2149; Istituto Nazionale di Fisica Nucleare, Italy; Ministry of Development of Turkey under Contract No. DPT2006K-120470; National Science and Technology fund; STFC (United Kingdom); The Royal Society, UK under Contracts No. DH140054, DH160214; The Swedish Research Council; U.S. Department of Energy under Contract No. DE-FG02-05ER41374.

[a]Also at the Moscow Institute of Physics and Technology, Moscow 141700, Russia.
[b]Also at the Novosibirsk State University, Novosibirsk, 630090, Russia.
[c]Also at the NRC “Kurchatov Institute”, PNPI, 188300, Gatchina, Russia.
[d]Also at Goethe University Frankfurt, 60323 Frankfurt am Main, Germany.
[e]Also at Key Laboratory for Particle Physics, Astrophysics and Cosmology, Ministry of Education; Shanghai Key Laboratory for Particle Physics and Cosmology; Institute of Nuclear and Particle Physics, Shanghai 200240, People’s Republic of China.
[f]Also at Key Laboratory of Nuclear Physics and Ion-beam Application (MOE) and Institute of Modern Physics, Fudan University, Shanghai 200443, People’s Republic of China.
[g]Also at State Key Laboratory of Nuclear Physics and Technology, Peking University, Beijing 100871, People’s Republic of China.
[h]Also at School of Physics and Electronics, Hunan University, Changsha 410082, China.
[i]Also at Guangdong Provincial Key Laboratory of Nuclear Science, Institute of Quantum Matter, South China Normal University, Guangzhou 510006, China.
[j]Also at Frontiers Science Center for Rare Isotopes, Lanzhou University, Lanzhou 730000, People’s Republic of China.
[k]Also at Lanzhou Center for Theoretical Physics, Lanzhou University, Lanzhou 730000, People’s Republic of China.
[l]Also at the Department of Mathematical Sciences, IBA, University Road, Karachi, 75270, Pakistan.

[1] N. Brambilla, S. Eidelman, C. Hanhart, A. Nefediev, C. P. Shen, C. E. Thomas, A. Vairo, and C. Z. Yuan, Phys. Rep. **873**, 1 (2020).
[2] F. K. Guo, C. Hanhart, Ulf-G. Meißner, Q. Wang, Q. Zhao, and B.-S. Zou, Rev. Mod. Phys. **90**, 015004 (2018).
[3] H. X. Chen, W. Chen, X. Liu, and S. L. Zhu, Phys. Rep. **639**, 1 (2016).
[4] N. Brambilla *et al.*, Eur. Phys. J. C **71**, 1534 (2011).
[5] M. Ablikim *et al.* (BESIII Collaboration), Phys. Rev. Lett. **110**, 252001 (2013).
[6] M. Ablikim *et al.* (BESIII Collaboration), Phys. Rev. Lett. **111**, 242001 (2013).
[7] M. Ablikim *et al.* (BESIII Collaboration), Phys. Rev. Lett. **112**, 022001 (2014).
[8] M. Ablikim *et al.* (BESIII Collaboration), Phys. Rev. Lett. **112**, 132001 (2014).
[9] M. Ablikim *et al.* (BESIII Collaboration), Phys. Rev. Lett. **113**, 212002 (2014).

[10] M. Ablikim *et al.* (BESIII Collaboration), Phys. Rev. Lett. **115**, 112003 (2015).
[11] M. Ablikim *et al.* (BESIII Collaboration), Phys. Rev. Lett. **115**, 182002 (2015).
[12] M. Ablikim *et al.* (BESIII Collaboration), Phys. Rev. D **92**, 092006 (2015).
[13] M. Ablikim *et al.* (BESIII Collaboration), Phys. Rev. Lett. **115**, 222002 (2015).
[14] Z. Q. Liu *et al.* (Belle Collaboration), Phys. Rev. Lett. **110**, 252002 (2013); **111**, 019901(E) (2013).
[15] T. Xiao, S. Dobbs, A. Tomaradze, and K. K. Seth, Phys. Lett. B **727**, 366 (2013).
[16] M. B. Voloshin, Phys. Lett. B **798**, 135022 (2019).
[17] S. H. Lee, M. Nielsen, and U. Wiedner, J. Korean Phys. Soc. **55**, 424 (2009).
[18] J. Ferretti and E. Santopinto, J. High Energy Phys. 04 (2020) 119.
[19] J. M. Dias, X. Liu, and M. Nielsen, Phys. Rev. D **88**, 096014 (2013).
[20] D. Y. Chen, X. Liu, and T. Matsuki, Phys. Rev. Lett. **110**, 232001 (2013).
[21] M. Ablikim *et al.* (BESIII Collaboration), Phys. Rev. Lett. **126**, 102001 (2021).
[22] L. Meng, B. Wang, and S. L. Zhu, Phys. Rev. D **102**, 111502(R) (2020).
[23] B. D. Wan and C. F. Qiao, Nucl. Phys. **B968**, 115450 (2021).
[24] Z. Yang, X. Cao, F. K. Guo, J. Nieves, and M. P. Valderrama, Phys. Rev. D **103**, 074029 (2021).
[25] L. Maiani, A. D. Polosa, and V. Riquer, Sci. Bull. **66**, 1616 (2021).
[26] L. Meng, B. Wang, G. J. Wang, and S. L. Zhu, Sci. Bull. **66**, 2065 (2021).
[27] R. Aaij *et al.* (LHCb Collaboration), Phys. Rev. Lett. **127**, 082001 (2021).
[28] M. Ablikim *et al.* (BESIII Collaboration), arXiv.2205.04809.
[29] M. Ablikim *et al.* (BESIII Collaboration), Nucl. Instrum. Methods Phys. Res., Sect. A **614**, 345 (2010).
[30] C. H. Yu *et al.*, in *Proceedings of IPAC2016, Busan, Korea* (2016), p. TUYA01.
[31] M. Ablikim *et al.* (BESIII Collaboration), Chin. Phys. C **44**, 040001 (2020).
[32] S. Agostinelli *et al.* (GEANT4 Collaboration), Nucl. Instrum. Methods Phys. Res., Sect. A **506**, 250 (2003).
[33] S. Jadach, B. F. L. Ward, and Z. Was, Phys. Rev. D **63**, 113009 (2001); Comput. Phys. Commun. **130**, 260 (2000).
[34] D. J. Lange, Nucl. Instrum. Methods Phys. Res., Sect. A **462**, 152 (2001); R. G. Ping, Chin. Phys. C **32**, 599 (2008).
[35] P. Z. Zyla *et al.* (Particle Data Group), Prog. Theor. Exp. Phys. **2020**, 083C01 (2020) and 2021 update.
[36] J. C. Chen, G. S. Huang, X. R. Qi, D. H. Zhang, and Y. S. Zhu, Phys. Rev. D **62**, 034003 (2000); R. L. Yang, R. G. Ping, and H. Chen, Chin. Phys. Lett. **31**, 061301 (2014).
[37] E. Richter-Was, Phys. Lett. B **303**, 163 (1993).
[38] M. Ablikim *et al.* (BESIII Collaboration), Chin. Phys. C **43**, 031001 (2019).
[39] See Supplemental Material at http://link.aps.org/supplemental/10.1103/PhysRevLett.129.112003 for additional analysis information.
[40] J. A. Rice, *Mathematical Statistics and Data Analysis* (Duxbury Press, Belmont, CA, 2007).
[41] F. Jegerlehner, Il Nuovo Cimento C **034S1**, 31 (2011).